Journal of Animal Science, 2020, Vol. 98, No. 10, 1–13

doi:10.1093/jas/skaa328
Advance Access publication October 7, 2020
Received: 25 August 2020 and **Accepted:** 30 September 2020
Molecular Nutrition

MOLECULAR NUTRITION

Protective effects of pterostilbene against hepatic damage, redox imbalance, mitochondrial dysfunction, and endoplasmic reticulum stress in weanling piglets

Hao Zhang,[†,‡,‖] Yanan Chen,[†] Yue Li,[$] Peilu Jia,[†] Shuli Ji,[†] Yueping Chen,[†] and Tian Wang[†,1]

[†]College of Animal Science & Technology, Nanjing Agricultural University, Nanjing, Jiangsu 210095, China, [‡]Postdoctoral Research Station of Clinical Veterinary Medicine, College of Veterinary Medicine, Nanjing Agricultural University, Nanjing, Jiangsu 210095, China, [‖]Shanghai Key Laboratory of Veterinary Biotechnology, Shanghai 200240, China, [$]Institute of Animal Science, Jiangsu Academy of Agricultural Sciences, Nanjing 210014, China

[1]Corresponding author: tianwangnjau@163.com

ORCiD number: 0000-0002-9038-5009 (T. Wang).

Abstract

This investigation evaluated the potential of natural antioxidants, pterostilbene (**PT**) and its parent compound resveratrol (**RSV**), to alleviate hepatic damage, redox imbalance, mitochondrial dysfunction, and endoplasmic reticulum (**ER**) stress in early-weaned piglets. A total of 144 suckling piglets were randomly assigned to four treatments (six replicates per group, $n = 6$): 1) sow reared, 2) early weaned and fed a basal diet, 3) early weaned and fed the basal diet supplemented with 300 mg/kg PT, or with 4) 300 mg/kg RSV. Early weaning increased plasma alanine aminotransferase ($P = 0.004$) and aspartate aminotransferase ($P = 0.009$) activities and hepatic apoptotic rate ($P = 0.001$) in piglets compared with the sow-reared piglets. Early weaning decreased hepatic adenosine triphosphate (**ATP**; $P = 0.006$) content and mitochondrial complexes III ($P = 0.019$) and IV activities ($P = 0.038$), but it increased superoxide anion accumulation ($P = 0.026$) and the expression levels of ER stress markers, such as glucose-regulated protein 78 ($P < 0.001$), CCAAT/enhancer-binding protein-homologous protein ($P = 0.001$), and activating transcription factor (**ATF**) 4 ($P = 0.006$). PT was superior to RSV at mitigating liver injury and oxidative stress after early weaning, as indicated by decreases in the number of apoptotic cells ($P = 0.036$) and the levels of superoxide anion ($P = 0.002$) and 8-hydroxy-2 deoxyguanosine ($P < 0.001$). PT increased mitochondrial deoxyribonucleic acid content ($P = 0.031$) and the activities of citrate synthase ($P = 0.005$), complexes I ($P = 0.004$) and III ($P = 0.011$), and ATP synthase ($P = 0.041$), which may contribute to the mitigation of hepatic ATP deficit ($P = 0.017$) in the PT-treated weaned piglets. PT also prevented increases in the ER stress marker and ATF 6 expression levels and in the phosphorylation of inositol-requiring enzyme 1 alpha caused by early weaning ($P < 0.05$). PT increased sirtuin 1 activity ($P = 0.031$) in the liver of early-weaned piglets than those in the early-weaned piglets fed a basal diet. In conclusion, PT supplementation alleviates liver injury in weanling piglets probably by inhibiting mitochondrial dysfunction and ER stress.

Key words: early weaning, endoplasmic reticulum stress, liver injury, mitochondrial dysfunction, piglet, pterostilbene

Abbreviations

8-OHDG	8-hydroxy-2 deoxyguanosine
ALT	alanine aminotransferase
AST	aspartate aminotransferase
ATP	adenosine triphosphate
CAT	catalase
DAPI	4′-6-diamidino-2-phenylindole
DHE	dihydroethidium
ER	endoplasmic reticulum
ETC	electron transfer chain
GPx	glutathione peroxidase
GST	glutathione S-transferase
H&E	hematoxylin and eosin
HRP	horseradish peroxidase
MDA	malondialdehyde
mtD-loop	mitochondrial D-loop
	mtDNA, mitochondrial deoxyribonucleic acid
NRF1	nuclear respiratory factor 1
NRF2	nuclear factor erythroid 2-related factor 2
OXPHOS	oxidative phosphorylation
PBS	phosphate-buffered saline
PT	pterostilbene
RSV	resveratrol
SOD	superoxide dismutase
TBS	tris-buffered saline
TCA	tricarboxylic acid
TEM	transmission electron microscopy
TUNEL	terminal deoxynucleotidyl transferase-mediated dUTP nick-end labeling
UPR	unfolded protein response
W-RSV	piglets fed a resveratrol-supplemented diet from 21 to 28 d of age
XBP1	X-box-binding protein 1

Introduction

Intensive swine production depends on high stocking densities and high yield, but these requirements increase the exposure risk of piglets to various stressful events and especially weaning stress. Early weaning is one of the most stressful periods for piglets and imposes a series of stressors resulting from dietary, physiological, and environmental changes that can lead to postweaning growth checks and inferior resistance to diseases (Sutherland et al., 2006; Campbell et al., 2013).

The liver, as the largest internal organ, is vulnerable to damage at weaning because of its functional immaturity and continuous exposure to intestinally derived pathogens and toxins (Seki and Schnabl, 2012). Recent evidence demonstrates an increase in oxidative damage in the liver of weanling piglets, an outcome that occurs when prooxidants overwhelm the cellular antioxidant capacity (Luo et al., 2016; Novais et al., 2020). Abrupt weaning evokes free radical overproduction and perturbs cellular antioxidant mechanisms, resulting in oxidative damage to biological substrates, including nucleic acids, proteins, and lipids (Zhu et al., 2012; Yin et al., 2014; Luo et al., 2016; Novais et al., 2020). The biological damage inflicted by oxidative stress is deleterious to the normal liver functions, which included nutrient metabolism, toxin clearance, and systemic defense. Oxidative stress has also been implicated in the escalating disease outbreaks in swine production (Vollmar and Menger, 2009). In this regard, a need exists for the development of strategies that facilitate natural defense mechanisms against oxidative damage to ensure the functionality of the liver during the stressful practice of early weaning.

One strategy that can reduce early weaning stress is dietary supplementation with antioxidants. The stilbenes, primarily found in grapes, berries, and peanuts, are a promising class of bioactive botanical compounds that exhibit promising health benefits by their antioxidant, anti-inflammatory, and hepatoprotective actions (Vladislav et al., 2006; Price et al., 2012; Zhang et al., 2020a). The best-studied stilbene is resveratrol (**RSV**), but RSV has several pharmacological defects, including a short half-life, extensive phase II metabolism, and poor bioavailability when administered orally (Baur and Sinclair, 2006; Choo et al., 2014; Rauf et al., 2017). These defects, therefore, limit the potential usefulness of RSV as a hepatoprotective agent in animal production. However, its naturally occurring dimethylether analog, pterostilbene (**PT**), has been attracting increasing attention as a dietary antioxidant with greater bioavailability and hepatic stability (Song et al., 2019; Wu et al., 2020; Zhang et al., 2020a).

The dimethoxy structure that distinguishes PT from RSV decreases the possibility of phase II reactions, thereby endowing PT with a slower clearance, a more abundant plasma exposure, and a longer elimination half-life (Yeo et al., 2013). The partial methylation also enhances the lipophilicity of PT to promote its membrane permeability and biological potency (Choo et al., 2014). Notably, orally administered PT exhibits abundant distribution to the liver (Choo et al., 2014), raising the possibility that PT may be a favorable candidate for further development as a therapeutic. However, the possibility that PT might alleviate weaning-induced liver injury has not been investigated. The aim of the present study was, therefore, to compare PT to its parent compound RSV for its effects on hepatic damage, redox status, and mitochondrial and endoplasmic reticulum (**ER**) function in weanling piglets.

Materials and Methods

Animals, diet, and housing

The animal experimentation and the corresponding protocols performed in this study (Permit number SYXK-2017-0027) complied with the guidelines of the Nanjing Agricultural University Institutional Animal Care and Use Committee. In total, 144 male suckling piglets (Duroc × [Landrace × Yorkshire]) were selected at age 21 d and then randomly assigned to four treatment groups (six replicates per group, $n = 6$): a sow-reared group (**SR-CON**), a weaned group fed a basal diet (**W-CON**), a weaned group fed a diet supplemented with 300 mg/kg of PT (**W-PT**), and a weaned group fed a diet supplemented with 300 mg/kg RSV (**W-RSV**). The SR-CON piglets were retained in the farrowing pens and were nursed by the sows until 28 d of age, whereas the remaining groups were moved to the weaner unit and fed the experimental diets. The dosages of PT and RSV used were selected according to the findings of previous investigations (Zhang et al., 2015; Gan et al., 2019). Dietary ingredients and the nutrient contents of the basal diet are presented in Supplementary Table S1. Feed and water were available ad libitum.

Sample collection

At the end of the feeding experiment, one piglet was randomly selected from each replicate (24 piglets in total). The selected piglets were euthanized by exsanguination after electrical stunning, and liver tissue was immediately collected from the left lobes. A portion of each liver sample was fixed in 4% paraformaldehyde (#P1110; Solarbio, Beijing, China), 2.5% glutaraldehyde (#G7776; Sigma-Aldrich, St. Louis, MO, USA), and optimal cutting temperature medium (#4583; Solarbio) for subsequent analyses. Approximately, 10 g of the fresh liver was collected from the same position for the isolation of mitochondria. The remaining liver tissues were stored at –80 °C until biochemical assays.

Plasma aminotransferase activities

Circulating alanine aminotransferase (**ALT**; #C009-2-1) and aspartate aminotransferase (**AST**; #C010-2-1) activities were determined by colorimetric methods using commercial kits (Nanjing Jiancheng Institute of Bioengineering Nanjing, Jiangsu, China).

Histopathology

After fixation in 4% paraformaldehyde for 24 h, the liver specimens were dehydrated, embedded in paraffin, cut into 5 μm sections, and stained with hematoxylin and eosin (**H&E**). Histological fields were randomly selected and images were captured with a light microscope (Nikon Eclipse 80i; Nikon, Tokyo, Japan). Histopathological alterations were evaluated by a histopathologist blinded to the group distribution.

Apoptosis

The number of apoptotic liver cells was determined with a One-step Terminal Deoxynucleotidyl Transferase-mediated dUTP Nick-end Labeling (**TUNEL**) Assay Kit (#A113-03; Vazyme, Nanjing, Jiangsu, China) according to the manufacturer's instructions. Briefly, the liver sections (5 μm) were pretreated with 20 μg/mL proteinase K at 25 °C for 15 min, followed by incubation with the TUNEL reagents in the dark at 37 °C for 1 h. The nuclei were identified by staining with 4′-6-diamidino-2-phenylindole (**DAPI**) dissolved in anti-fade mounting medium (#P0131; Beyotime, Shanghai, China). The number of TUNEL-labeled cells in 15 randomly fields per section was quantified by a blinded observer using a fluorescence microscope (Nikon Eclipse 80i).

Transmission electron microscopy

Liver tissues were fixed overnight at 4 °C in 2.5% glutaraldehyde in 0.1 M sodium cacodylate buffer and then post-fixed for 1 h in 1% osmium tetroxide. After dehydration using standard protocols, the specimens were embedded in epoxy resin and ultrathin sections were prepared (Reichert Ultracut microtome, Leica, Deerfield, IL, USA) and imaged by a TEM (Hitachi H-7650, Tokyo, Japan).

Immunohistochemical staining

Paraffin-embedded liver sections (5 μm) were deparaffinized, rehydrated, and rinsed for 10 min in 0.1 M phosphate-buffered saline (**PBS**). Endogenous peroxidase activity was inhibited by treatment of the sections with 3% hydrogen peroxide for 30 min in the dark. The sections were then incubated with a primary rabbit polyclonal antibody against glucose-regulated protein 78 (**GRP78**; #11587-1-AP; Proteintech, Chicago, IL, USA) overnight in a humid chamber. After washing with PBS, the sections were incubated with a horseradish peroxidase (**HRP**)-conjugated goat anti-rabbit secondary antibody (#SA00001-2; Proteintech) at 25 °C for 1 h. The dilution for both antibodies was 1:100 in Tris-buffered saline (**TBS**) and 5% skimmed milk. The color of HRP was developed with a Diaminobenzidene HRP Color Development Kit (#P0203; Beyotime) and observed by light microscopy (Nikon Eclipse 80i).

Superoxide anion levels

Hepatic superoxide accumulation was detected with a fluorescent dye, dihydroethidium (**DHE**; #309800; Sigma-Aldrich, St. Louis, MO, USA), based on the methods described by Yueh et al. (2014). DHE is an oxidant-sensitive fluorescent probe that can interact with intracellular superoxide anion to produce a fluorescent signal (Zhao et al., 2003). Briefly, liver cryosections (5 μm) were incubated with 10 μM DHE at 37 °C for 30 min. Cells staining positive for the oxidized dye were detected by fluorescence microscopy (Nikon Eclipse 80i). Ten random fields per section were quantified using Image J software (NIH, Baltimore, MD, USA).

Redox status

Hepatic superoxide dismutase (**SOD**; #A001-1-2), glutathione peroxidase (**GPx**; #A005-1-2), and catalase (**CAT**; #A007-1-1) activities and malondialdehyde (**MDA**; #A003-1-2) content were measured using colorimetric kits (Nanjing Jiancheng Institute of Bioengineering) according to the manufacturer's protocols. Glutathione S-transferase (**GST**; #GST-2-W) activity was measured based on ultraviolet spectrophotometry using a detection assay kit (Suzhou Comin Biotechnology Co., Ltd.). The concentration of hepatic 8-hydroxy-2 deoxyguanosine (**8-OHDG**; #589320-96S) was determined by an enzyme-linked immunosorbent assay using a commercial kit (Cayman Chemical; Ann Arbor, MI, USA).

Mitochondrial enzyme activities

A commercial kit was used to extract mitochondria from the fresh liver tissues (#SM0020; Solarbio). The protein content of the mitochondrial suspension was determined, and then the activities of citrate synthase (**CS**; #BC1065); electron transport chain complexes I (#BC0515), II (#BC3230), III (#BC3240), and IV (#BC0945); and adenosine triphosphate (**ATP**) synthase (#BC1445) were determined using colorimetric kits (Solarbio), following the manufacturer's guidelines.

Hepatic ATP content

The liver samples were weighed, ground, blended with boiling double-distilled H_2O, boiled for 30 min, and then centrifuged at 4,000 × *g* for 15 min. The resulting supernatant was collected, and the ATP content was determined with a commercial kit (Nanjing Jiancheng Institute of Bioengineering).

Mitochondrial deoxyribonucleic acid content

Total DNA was extracted from frozen liver samples with the TIANamp Genomic DNA kit (#DP304-03; Tiangen, Beijing, China). Real-time polymerase chain reaction (PCR) was used for the relative quantification of mitochondrial deoxyribonucleic acid (**mtDNA**) copy number using the QuantStudio 5 Real-time PCR System (Applied Biosystems, Life Technologies, CA, USA) and the ChamQ SYBR qPCR master mix (#Q311-02; Vazyme), according to the manufacturer's recommended protocols. The mitochondrial D-loop (**mtD-loop**) was selected as the indicator of mtDNA, and beta actin (**ACTB**), a marker of nuclear DNA, was used as the internal control. The primers were as follows. The

mtD-loop forward: 5′-GATCGTACATAGCACATATCATGTC-3′, reverse: 5′- GGTCCTGAAGTAAGAACCAGATG-3′. The ACTB forward: 5′-CCCCTCCTCTCTTGCCTCTC-3′; reverse: 5′-AAAAGTCCTAGGAA AATGGCAGAAG-3′. The $2^{-\Delta\Delta Ct}$ method was performed to calculate the copy number of mtDNA (Livak and Schmittgen, 2001).

Sirtuin 1 activity

Nuclear extracts from fresh liver tissues were prepared using a Nuclear Protein Extraction Kit (#P0028; Beyotime). Sirtuin 1 (**SIRT1**) activity in the hepatic nuclear protein was evaluated using a commercial assay kit obtained from Genmed (#50287.2; Shanghai, China). The experimental procedures were performed following the instructions of the manufacturers.

Gene expression

The methods for isolation and quality determination of total RNA and for the synthesis of complementary DNA were as described previously (Zhang et al., 2020b). Real-time PCR was carried out with SYBR Green reagent to measure the expression of SIRT1, peroxisome proliferation-activated receptor gamma co-activator 1 alpha (**PGC-1α**), mitochondrial transcription factor A (**TFAM**), nuclear respiratory factor 1 (**NRF1**), estrogen-related receptor alpha (**ERRα**), peroxisome proliferator-activated receptor alpha (**PPARα**), carnitine palmitoyltransferase 1A (**CPT1A**), GRP78, GRP94, CCAAT/enhancer-binding protein-homologous protein (**CHOP**), activating transcription factor 4 (**ATF4**), ER oxidoreductase 1 alpha (**ERO1A**), ER oxidoreductase 1 beta (**ERO1B**), glyceraldehyde-3-phosphate dehydrogenase, and ACTB, following the manufacturer's recommended protocols. Fluorescence measurements were made using a QuantStudio 5 Real-time PCR System instrument (Applied Biosystems). Supplementary Table S2 presents the details of the primer sequences used in this work. The cDNA input levels of each sample were normalized using its ACTB expression. The $2^{-\Delta\Delta Ct}$ method was used for comparisons between the groups (Livak and Schmittgen, 2001).

Western blotting

Protein extracts were prepared by lysing approximately 100 mg of liver samples in 1:9 (wt/vol) lysis buffer containing protease and phosphatase inhibitors. Nuclear protein was extracted from fresh liver samples as mentioned above. After centrifugation, the supernatant was mixed with sodium dodecyl sulfate sample buffer and then boiled for 5 min. The protein concentration was determined and an equal amount of isolated protein was separated by sodium dodecyl sulfate-polyacrylamide gel electrophoresis. The separated proteins were then transferred to Immobilon-P transfer membranes. The membranes were blocked with 5% skimmed dry milk in TBS combined with 0.2% Tween-20 for 2 h at room temperature. The membranes were then immunoblotted using rabbit polyclonal antibodies against nuclear factor erythroid 2-related factor 2 (**NRF2**; #ab92946; Abcam, Cambridge, MA, USA), histone H3 (#5192S; CST, Danvers, MA, USA), GRP78 (#11587-1-AP; Proteintech), inositol-requiring enzyme 1 alpha (**IRE1α**; #bs8680R; Bioss Biotechnology, Beijing, China), protein kinase RNA-like ER kinase (**PERK**; #24390-1-AP; Proteintech), phospho-IRE1α (Ser^{726}; #bs-4308R; Bioss Biotechnology), phospho-PERK (Thr^{980}; #bs-3330R; Bioss Biotechnology), ATF6 (#24169-1-AP; Proteintech), and ACTB (#20536-1-AP; Proteintech). Immunoreactivity was detected with a goat anti-rabbit secondary antibody (#SA00001-2; Proteintech) and then developed using an enhanced chemiluminescence HRP substrate (#WBKLS0100; Millipore, Bedford, MA, USA). The gray scale values of the bands were measured using the Gel-Pro Analyzer program, version 4.0 (Media Cybernetics, Inc., MD, USA).

Statistical analysis

Data were analyzed using the IBM SPSS Statistics software, version 22.0. Statistical differences were assessed using one-way analysis of variance, followed by the Tukey's post hoc test for the comparison between two groups. The criterion for the statistical significance was $P < 0.05$. All data are presented as mean values and standard errors (mean ± SE).

Results

Hepatic injury

To monitor the severity of hepatic damage induced by early weaning, we first carried out a histopathological analysis of the livers of these piglets and measured the levels of liver cell apoptosis. Livers from the SR-CON group showed normal hepatocyte architecture with well-preserved cytoplasm (Figure 1A). A few vacuoles were seen in the cytoplasm of hepatocytes from the W-CON piglets, along with mild disorganization of the parenchyma. These defects were completely absent in the PT-supplemented piglet livers, but only moderately reduced by RSV supplementation. The W-CON piglets exhibited an increase in hepatic apoptosis ($P = 0.001$) when compared with the SR-CON piglets (Figure 1B and Table 1). The activities of plasma ALT ($P = 0.004$) and AST ($P = 0.009$) were also substantially higher in the W-CON piglets than in their SR-CON counterparts. After the 1-wk feeding trial, PT supplementation prevented the appearance of increased plasma ALT activity ($P = 0.002$) and the greater number of hepatic apoptotic cells ($P = 0.036$) induced by early weaning. However, these effects were not prevented by supplementation with RSV ($P > 0.05$).

Hepatic oxidative stress

Since oxidative stress has been reported to be increased in piglets at weaning (Zhu et al., 2012; Yin et al., 2014; Luo et al., 2016; Novais et al., 2020), we tested the accumulation of superoxide anion and the contents of MDA (main end product of lipid peroxidation) and 8-OHDG (the predominant form of free radical-induced lesions of DNA) in the liver of piglets. Early weaning resulted in dramatic increases in superoxide accumulation ($P = 0.026$) in the liver (Figure 2A and B). The levels of hepatic MDA ($P = 0.001$) and 8-OHDG ($P < 0.001$) were significantly higher in the W-CON piglets than in the SR-CON piglets (Figure 2C and D). Treatment with PT prevented the early weaning-induced accumulation of superoxide anion ($P = 0.002$) in the liver. PT effectively inhibited the increases in 8-OHDG content ($P < 0.001$) induced by early weaning. The hepatic levels of MDA ($P = 0.012$) and 8-OHDG ($P < 0.001$) were also higher in the piglets fed the RSV-supplemented diet than in the piglets nursed by the sows.

Hepatic antioxidant capacity

Next, we analyzed the activities of hepatic antioxidant enzymes and the levels of NRF2 nuclear translocation. The activities of hepatic SOD ($P = 0.029$) and CAT ($P = 0.009$) were higher in the W-CON group than in the SR-CON group (Table 2). Both PT ($P = 0.004$) and RSV ($P = 0.001$) treatments suppressed this early weaning-induced increase in hepatic CAT activity. No difference

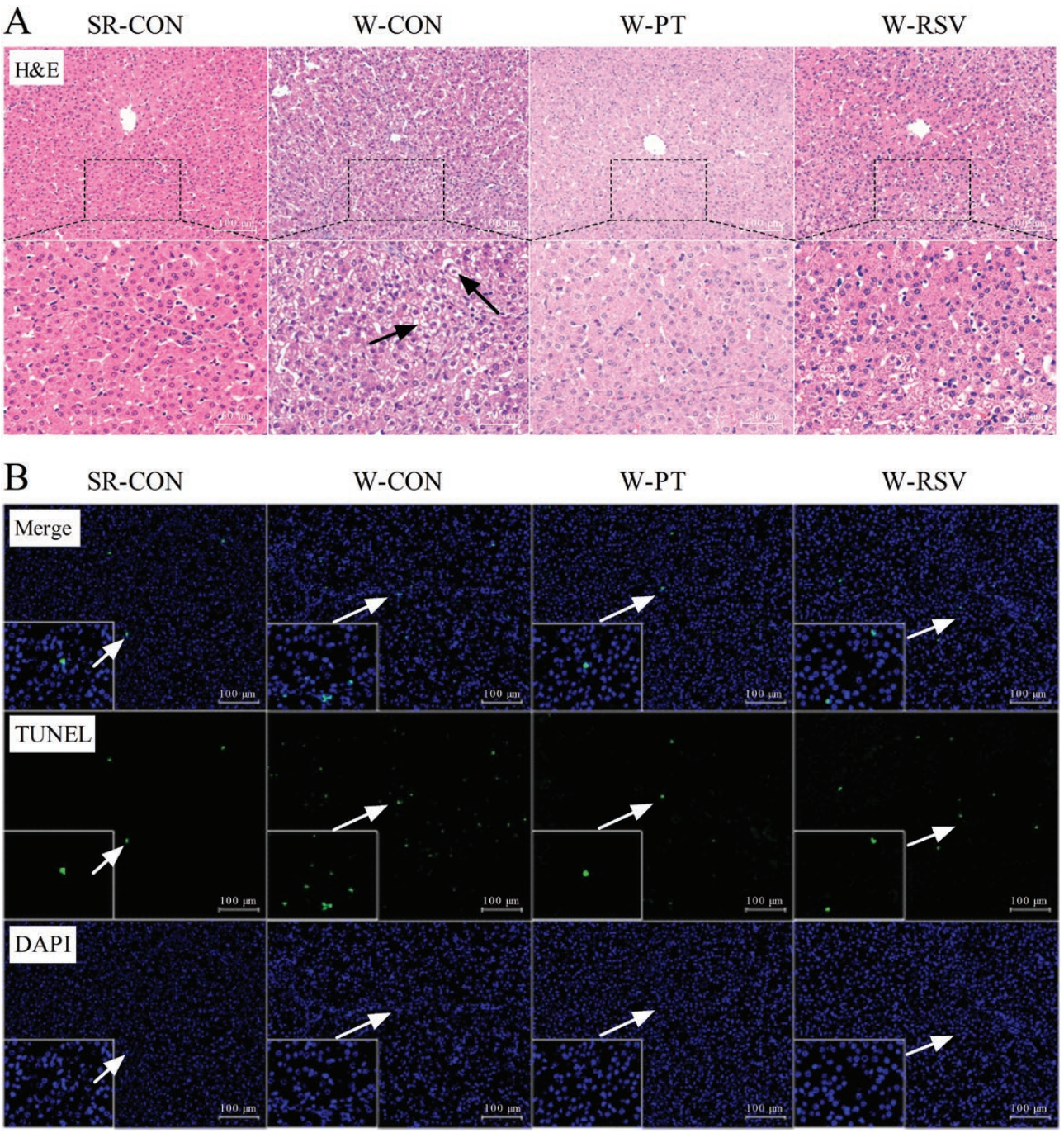

Figure 1. Effects of PT and RSV supplementation on hepatic morphology and the number of apoptotic cells in weanling piglets. (A) Representative histopathological images of H&E staining (200× and 400× magnification); (B) Representative micrographs of TUNEL staining (200× and 1,000× magnification).

Table 1. Effects of PT and RSV supplementation on plasma aminotransferase activities and hepatic apoptosis in weanling piglets[1,2]

Items	SR-CON	W-CON	W-PT	W-RSV
Plasma				
ALT, U/L	12.63 ± 1.36	23.83 ± 2.51[a]	11.70 ± 0.89[b]	19.17 ± 2.59
AST, U/L	19.70 ± 3.01	46.76 ± 8.15[a]	26.97 ± 5.49	33.10 ± 2.55
Liver				
TUNEL-positive cells, %	0.78 ± 0.16	2.18 ± 0.24[a]	1.29 ± 0.25[b]	1.54 ± 0.19

[1]Values are means ± SE, $n = 6$.
[2]SR-CON, sow-reared control; W-CON, weaned group fed basal diet; W-PT, weaned group fed basal diet supplemented with 300 mg/kg PT; W-RSV, weaned group fed basal diet supplemented with 300 mg/kg RSV.
[a]$P < 0.05$ compared with SR-CON group; [b]$P < 0.05$ compared with W-CON group.

was observed for GPx or GST activities in the four groups ($P > 0.05$). Piglets in the W-PT group showed a significant increase in the amount of nuclear NRF2 protein ($P = 0.001$; Figure 3) compared with those in the SR-CON group. However, RSV did not affect the accumulation of nuclear NRF2 protein in the liver of W-RSV piglets compared with either SR-CON or W-CON group ($P > 0.05$).

Hepatic energy metabolism

Energy homeostasis is susceptible to reactive oxygen species (ROS)-mediated oxidative stress (Pike et al., 2011; Wu et al., 2014). We accordingly tested the efficiency of mitochondrial oxidative metabolism and ATP production in the liver. Hepatic ATP content ($P = 0.006$) and mitochondrial electron transfer chain (**ETC**) complexes III ($P = 0.019$) and IV activities ($P = 0.038$) were lower in the W-CON piglets than in the SR-CON piglets (Table 3). Treatment with PT significantly increased hepatic ATP concentration ($P = 0.017$) and the activities of mitochondrial CS ($P = 0.005$), complexes I ($P = 0.004$) and III ($P = 0.011$), and ATP synthase ($P = 0.041$) in the weanling piglets compared with the basal diet. The activity of hepatic complex I ($P = 0.025$) was also higher in the RSV-treated weaned piglets than in the piglets fed the unsupplemented basal diet.

Hepatic mtDNA content and SIRT1 activity

To further investigate the mechanisms by which stilbenes stimulated hepatic energy metabolism, the analyses of hepatic mtDNA content and SIRT1 activity were performed. Early weaning of piglets had no effect on the hepatic mtDNA copy number or SIRT1 activity when compared with piglets nursed by the sows ($P > 0.05$; Figure 4). Dietary PT supplementation significantly increased the mtDNA content ($P = 0.031$) in the livers of early-weaned piglets compared with the SR-CON piglets. PT also elevated the activity of hepatic SIRT1 over that in the SR-CON ($P = 0.018$) or the W-CON piglets ($P = 0.031$). By contrast, RSV treatment had no effect on mtDNA content or SIRT1 activity ($P > 0.05$).

Hepatic genes expression

We then extended our analysis by examining the expression of genes related to mitochondrial biogenesis and energy metabolism. No difference was detected in the mRNA abundance of hepatic genes related to mitochondrial biogenesis or fatty acid oxidation in the SR-CON and W-CON groups ($P > 0.05$; Table 4). Supplementation of the weanling piglet diet with PT significantly increased the mRNA abundance of hepatic SIRT1 ($P = 0.024$) above that in the suckling piglets. PT also increased the expression levels of hepatic PPARα and CPT1A mRNA above that seen in the suckling piglets or the weanling piglets fed the unsupplemented basal diet ($P < 0.05$). PT supplementation also substantially upregulated the mRNA abundance of NRF1 ($P = 0.007$) and TFAM ($P = 0.030$) in the liver above that of weanling piglets fed the basal diet alone. By contrast, supplementation with RSV did not alter the mRNA levels of these genes ($P > 0.05$).

Hepatic ER stress

Disruption in the ER hemostasis has also been implicated in the development of liver damage associated with oxidative stress (Malhotra and Kaufman, 2007). We finally tested the severity of hepatic ER stress in piglets. Hepatocytes from the SR-CON group contained round nuclei, rod-shaped mitochondria, and abundant and well-developed ER (Figure 5A). By contrast, the ER of W-CON piglets exhibited obvious signs of ultrastructural injury, as characterized by dilated cisternae, which were rarely observed in the SR-CON piglets. Dietary supplementation with the two stilbenes, and particularly with PT, suppressed this ER swelling in the hepatocytes. Immunohistochemical and Western blot analyses indicated that early weaning significantly increased the expression of hepatic GRP78 ($P = 0.047$), a sensitive marker of ER stress (Figure 5B and C). The mRNA levels of hepatic GRP78 ($P < 0.001$), CHOP ($P = 0.001$), ATF4 ($P = 0.006$), and ERO1A ($P = 0.006$) were all increased in the W-CON group above the levels observed in the SR-CON group (Figure 5D). The phosphorylation of IRE1α ($P = 0.018$)

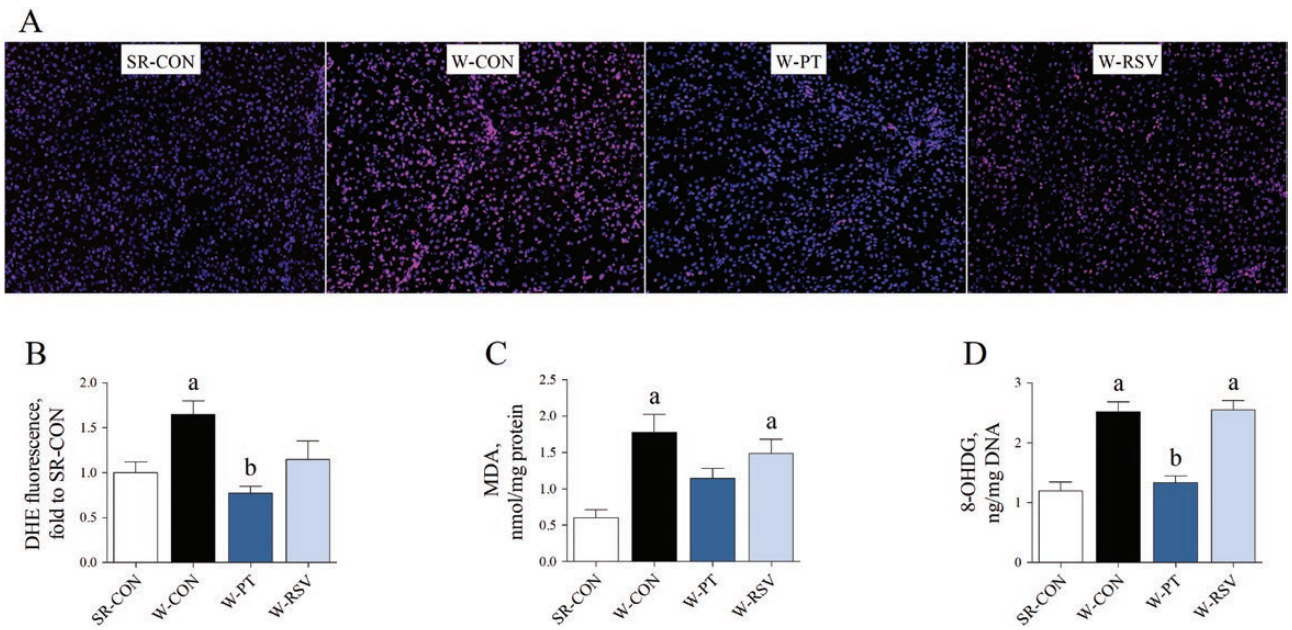

Figure 2. Effects of PT and RSV supplementation on hepatic oxidative stress in weanling piglets. (A and B) Hepatic superoxide anion levels measured with DHE fluorescent probe; (C) MDA content, and (D) 8-OHDG content. Values are represented as mean ± SE, $n = 6$. [a]Significant difference compared with SR-CON. [b]Significant difference compared with W-CON.

Table 2. Effects of PT and RSV supplementation on hepatic antioxidant enzyme activities in weanling piglets[1,2]

Items	SR-CON	W-CON	W-PT	W-RSV
SOD, U/mg protein	112.73 ± 6.12	155.13 ± 12.87[a]	134.82 ± 9.36	136.54 ± 9.67
GPx, U/mg protein	96.69 ± 9.86	71.79 ± 4.74	86.63 ± 9.80	77.21 ± 12.10
CAT, U/mg protein	151.40 ± 17.84	227.12 ± 15.18[a]	143.13 ± 3.86[b]	130.41 ± 18.04[b]
GST, U/mg protein	59.46 ± 2.74	66.07 ± 1.89	60.20 ± 1.29	67.76 ± 5.62

[1]Values are means ± SE, $n = 6$.
[2]SR-CON, sow-reared control; W-CON, weaned group fed basal diet; W-PT, weaned group fed basal diet supplemented with 300 mg/kg PT; W-RSV, weaned group fed basal diet supplemented with 300 mg/kg RSV.
[a]$P < 0.05$ compared with SR-CON group; [b]$P < 0.05$ compared with W-CON group.

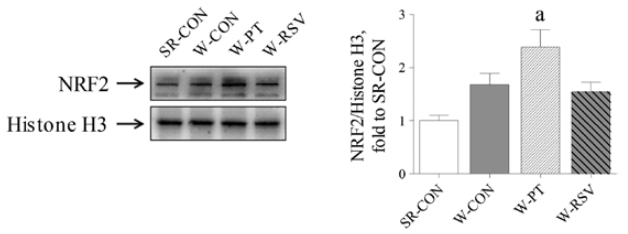

Figure 3. Effects of PT and RSV supplementation on the expression levels of nuclear NRF2 protein in the liver of piglets. Values are represented as mean ± SE, $n = 6$. [a]Significant difference compared with SR-CON.

and the protein content of ATF6 ($P = 0.031$) were also higher in the livers of the W-CON group than in the SR-CON group (Figure 5E and G). Supplementation with PT decreased the expression of GRP78 at both the mRNA ($P < 0.001$) and protein levels ($P = 0.014$). The mRNA levels of CHOP ($P = 0.002$), ATF4 ($P = 0.005$), and ERO1A ($P = 0.004$), the phosphorylation of IRE1α ($P = 0.002$), and ATF6 protein content ($P < 0.001$) were also reduced by PT supplementation to levels close to those in the sow-reared piglets. PT supplementation also increased the phosphorylation of hepatic PERK in the weanling piglets above those in either suckling piglets ($P = 0.057$) or piglets fed a basal diet ($P = 0.037$; Figure 5F). RSV treatment also decreased the hepatic GRP78 ($P < 0.001$) and ATF4 mRNA ($P = 0.002$) and IRE1α phosphorylation levels ($P = 0.031$).

Discussion

Early weaning of piglets is frequently accompanied with liver disorders and oxidative damage, but the underlying mechanism remains poorly explored (Luo et al., 2016; Novais et al., 2020). The findings presented here are the first to indicate that that early weaning results in hepatic mitochondrial dysfunction and ER stress that may be critical factors in the hepatic oxidative stress of piglets. Cellular redox status is closely linked to mitochondrial function and ER homeostasis, so disruption of any of these three elements, as often occurs at weaning, creates a vicious with eventual outcomes of cellular dysfunction and oxidative damage (Cao and Kaufman, 2013).

In the present study, the supplementation of the weanling piglet diet with PT alleviated the early-weaning hepatic damage and oxidative stress probably by suppressing mitochondrial dysfunction and ER stress. By contrast, supplementation with RSV at an equivalent dose failed to achieve a comparable protection, most likely reflecting the differences between RSV and PT in terms of oral bioavailability and hepatic stability (Yeo et al., 2013; Choo et al., 2014).

PT increased the expression and activity of hepatic SIRT1, a master regulator of metabolic homeostasis, mitochondrial function, and cellular resistance to stress (Li et al., 2011; Chang and Guarente, 2014). These alterations may contribute to the mitigation of hepatic dysfunction after PT treatment. For example, Price et al. (2012) have reported that SIRT1 is required for the protective effect of RSV on mitochondrial respiration and membrane potential. Likewise, other recent evidence has also indicated the importance of SIRT1 activation in the protective action of PT against acute and chronic liver disorders involving mitochondrial dysfunction and metabolic derangements (Liu et al., 2017; Song et al., 2019; Wu et al., 2020; Zhang et al., 2020a).

Several natural stilbenes, such as RSV and PT, can increase SIRT1 activity by facilitating the binding affinity between SIRT1 and its substrates (Hubbard et al., 2013; Zhang et al., 2020a). In the current work, PT was superior to RSV in terms of activating hepatic SIRT1 activity in weanling piglets. PT and RSV differ in their pharmacological properties, but an in vitro study further revealed that PT also has a distinct molecular docking mechanism with SIRT1. RSV simply interacts with Cys^{482} and Ser^{422} of SIRT1, whereas PT embeds nicely into the catalytic pocket of SIRT1 at Cys^{482} and Arg^{466} (Guo et al., 2016).

PT has also been reported to prevent the downregulation of SIRT1 induced by different harmful stimuli (Guo et al., 2016; Liu et al., 2019). Wu et al. (2020) further showed that PT promotes hepatic SIRT1 expression by suppressing its negative modulator microRNA-34a. These findings may explain the observed increases in hepatic SIRT1 mRNA abundance and activity by dietary PT supplementation in the present study. The activation of SIRT1 would be expected to confer protection that could facilitate mitochondrial energy metabolism. For instance, one effect of PT would be an improvement of CS activity, which would facilitate mitochondrial oxidative phosphorylation (**OXPHOS**) and increase ATP generation.

CS plays a vital role in the regulation of oxidative metabolism and ATP production, as it catalyzes the first committed step of the tricarboxylic acid (**TCA**) cycle (Cheng et al., 2016). Similar findings of increased CS activity were also observed in the PT-treated obese rats (Aguirre et al., 2016). Liu et al. (2019) have also shown that PT ameliorates the ATP depletion observed in H9c2 cells exposed to doxorubicin. Increased ATP production was also found in C2C12 myotubes after treatment with PT (Zheng et al., 2020). The findings presented here for weanling piglets further corroborate these previous findings, as PT improved the efficiency of the mitochondrial TCA cycle and OXPHOS in the liver of piglets and may have helped to alleviate the energy deficiency and liver disorders induced by early weaning.

A second PT effect was that it apparently enhanced hepatic mitochondrial biogenesis in early-weaned piglets, as indicated by the increase in mtDNA content in the W-PT group. PT has

Table 3. Effects of PT and RSV supplementation on hepatic ATP production and mitochondrial oxidative metabolism in weanling piglets[1,2]

Items	SR-CON	W-CON	W-PT	W-RSV
ATP, μmol/g wet weight	38.92 ± 5.54	18.88 ± 2.81[a]	36.56 ± 3.60[b]	29.03 ± 2.41
CS, U/mg protein	100.86 ± 5.64	63.39 ± 5.53	117.76 ± 16.74[b]	73.04 ± 7.36
Complex I, U/mg protein	5.41 ± 0.63	4.05 ± 0.55	7.26 ± 0.67[b]	6.58 ± 0.40[b]
Complex II, U/mg protein	8.32 ± 1.17	7.20 ± 1.24	9.70 ± 1.65	9.94 ± 0.62
Complex III, U/mg protein	8.56 ± 0.67	5.26 ± 0.60[a]	8.82 ± 0.67[b]	7.77 ± 0.88
Complex IV, U/mg protein	31.70 ± 2.80	17.79 ± 2.37[a]	20.52 ± 2.90	22.26 ± 4.81
ATP synthase, U/mg protein	31.94 ± 3.42	24.18 ± 1.99	37.51 ± 3.03[b]	30.06 ± 4.20

[1]Values are means ± SE, $n = 6$.
[2]SR-CON, sow-reared control; W-CON, weaned group fed basal diet; W-PT, weaned group fed basal diet supplemented with 300 mg/kg PT; W-RSV, weaned group fed basal diet supplemented with 300 mg/kg RSV.
[a]$P < 0.05$ compared with SR-CON group; [b]$P < 0.05$ compared with W-CON group.

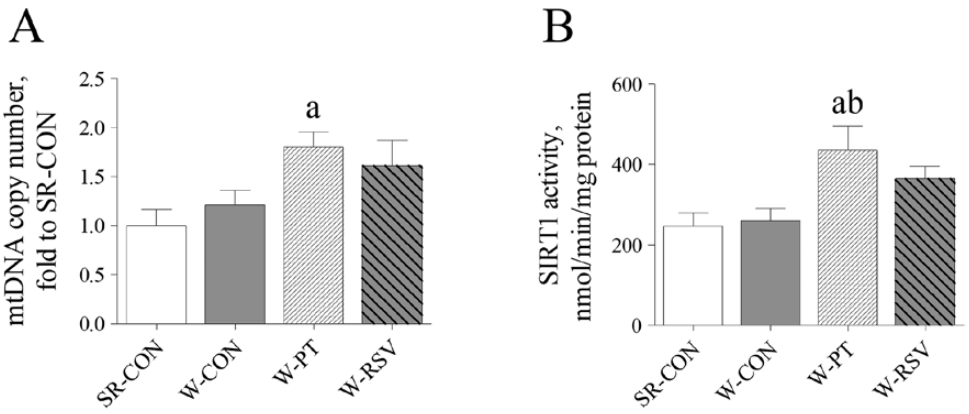

Figure 4. Effects of PT and RSV supplementation on hepatic mtDNA content (A) and SIRT1 activity (B) in weanling piglets. Values are represented as mean ± SE, $n = 6$. [a]Significant difference compared with SR-CON. [b]Significant difference compared with W-CON.

recently been reported to improve muscular mitochondrial biogenesis in rats that in turn are thought to facilitate the skeletal muscle adaptions shown by the rats in response to exercise training (Zheng et al., 2020). The mitochondrial genome content reflects the abundance of mitochondria within a cell and is regulated by a series of nuclear transcription factors and hormone nuclear receptors. Kosuru et al. (2018) have reported that PT improves mitochondrial biogenesis through its role in upregulating the expression levels of PGC-1α and complexes III and V subunits. SIRT1 facilitates mitochondrial biogenesis via PGC-1α, indicating that SIRT1 and PGC-1α both may be part of an upstream signaling axis that activates nucleus-encoded genes involved in mitochondrial metabolism (Brenmoehl and Hoeflich, 2013).

In the early-weaned piglet livers, dietary PT supplementation increased the mRNA abundance of NRF1, a downstream effector of the SIRT1/PGC-1α axis that plays an important role in the transcription of OXPHOS components and mitochondrial proteins (Aquilano et al., 2010). NRF1 is also responsible for the activation of TFAM, which is necessary for the transcription, replication, and maintenance of mtDNA (Kang et al., 2007). The upregulation of NRF1, as observed in the livers of the W-PT group, may account for the simultaneous increases in TFAM expression and mtDNA content. Notably, a rat model of metabolic derangements also showed that PT was more effective than RSV at preventing the downregulation of TFAM in the liver (Nirwane and Majumdar, 2016). A similar effect was also observed in the present early-weaned piglets, as the expression of hepatic TFAM was increased by supplementation with PT but not with RSV. Collectively, the findings in the present study indicate that PT may improve hepatic mitochondrial biogenesis in early-weaned piglets by stimulating SIRT1 signals and the expression of downstream NRF1 and TFAM.

A third PT effect revealed in the present study was that PT promoted the expression of hepatic PPARα and CPT1A. PPARα promotes fatty acid oxidation by increasing the transcriptional expression of several enzymes involved in fatty acid uptake, transport, and metabolism (Leone et al., 1999), while its downstream target, CPT1A, acts as a rate-limiting enzyme that controls long-chain fatty acid oxidation (Nakamura et al., 2014). The increased PPARα and CPT1A expression indicated a greater efficiency of fatty acid oxidation in the livers of the W-PT piglets, in agreement with the improvement in mitochondrial function and ATP production (Shen et al., 2008; Nakamura et al., 2014). Fatty acid oxidation is a major source of acetyl coenzyme A that fuels the mitochondrial TCA cycle and supports subsequent OXPHOS (Yang et al., 2014).

Available evidence has indicated that PT activates PPARα expression mostly through the activation of the SIRT1/PGC-1α axis. A signal interaction occurs in the cross talk between PPARα and the SIRT1/PGC-1α axis, and this effect may explain how PT can serve as a dual inducer for the transcriptional expression of PGC-1α and PPARα in streptozotocin-induced diabetic rats (Naik et al., 2017). By contrast, RSV did not affect the expression of PPARα, which may be attributed to the dosage used in the current study. Oral administration of PT at a low dose (5 mg/

Table 4. Effects of PT and RSV supplementation on the expression of hepatic genes related to mitochondrial biogenesis and fatty acid oxidation in weanling piglets[1,2]

Items	SR-CON	W-CON	W-PT	W-RSV
SIRT1	1.00 ± 0.18	1.16 ± 0.23	1.81 ± 0.17[a]	1.24 ± 0.13
PGC-1α	1.00 ± 0.13	0.61 ± 0.05	1.03 ± 0.11	0.95 ± 0.14
NRF1	1.00 ± 0.13	0.57 ± 0.03	1.36 ± 0.13[b]	0.93 ± 0.24
ERRα	1.00 ± 0.26	0.84 ± 0.09	0.78 ± 0.18	1.17 ± 0.39
TFAM	1.00 ± 0.15	0.82 ± 0.13	1.46 ± 0.15[b]	1.19 ± 0.16
PPARα	1.00 ± 0.09	1.08 ± 0.10	1.96 ± 0.24[ab]	1.20 ± 0.12
CPT1A	1.00 ± 0.31	0.81 ± 0.09	2.11 ± 0.14[ab]	0.74 ± 0.08

[1]Values are means ± SE, $n = 6$.
[2]SR-CON, sow-reared control; W-CON, weaned group fed basal diet; W-PT, weaned group fed basal diet supplemented with 300 mg/kg PT; W-RSV, weaned group fed basal diet supplemented with 300 mg/kg RSV.
[a]$P < 0.05$ compared with SR-CON group; [b]$P < 0.05$ compared with W-CON group.

kg body weight) rescued the downregulation of hepatic PPARα in estrogen-deficient rats chronically exposed to the aqueous extract of tobacco leaves, whereas a comparable effect for RSV was achieved at a dose of 40 mg/kg body weight (Nirwane and Majumdar, 2016).

PT serves as a potent agonist of PPARα probably through its direct docking interactions (Mizuno et al., 2008). Nagao et al. (2017) have demonstrated that PT dose-dependently increases the activity of PPARα in vitro, an effect that was absent in the RSV-treated group. The two methoxy groups of PT allow the formation of hydrogen bond interactions with PPARα at Ser^{280} and Tyr^{464}, which are regarded as the critical sites for PPARα activation (Mizuno et al., 2008). In this context, PT prevents obesity in rats by increasing energy metabolism and especially fat oxidation (Nagao et al., 2017). Therefore, the upregulation of PPARα after PT treatment may improve the availability of substrates for energy metabolism, thereby contributing to increases in mitochondrial CS, complexes I and III, and ATP synthase activities and in ATP content in the liver.

In addition to improving mitochondrial energy metabolism, PT also inhibited the overproduction of superoxide anion. Consistent with the present findings, animal models of cerebral ischemia-reperfusion injury show that PT can alleviate mitochondrial free radical accumulation and oxidative insults by increasing the activities of ETC complexes I and IV (Yang et al., 2016). Increases in mitochondrial complex activities, and particularly complexes I and III, may reduce the leakage of electrons from the ETC, thereby decreasing the reaction between free electrons and molecular oxygen and the resulting formation of superoxide anion (Korla, 2016). PT also has the potential to prevent the collapse of the mitochondrial membrane potential and inhibit the translocation of cytochrome c from the mitochondria to the cytoplasm, thereby conferring protection to mitochondrial homeostasis under adverse situations (Yang et al., 2017).

The mechanism by which PT inhibits free radical production may involve its ability to regulate cellular redox status, as PT is a potent scavenger of various free radicals. The present study also found that PT had the potential to promote the nuclear import of NRF2, a crucial factor that regulates cellular defense mechanisms. PT has been demonstrated to be a potent agonist of NRF2 (Chiou et al., 2011; Bhakkiyalakshmi et al., 2016). Similarly, we recently found that PT activated hepatic NRF2 and its downstream manganese SOD in an acute oxidative stress model induced by diquat, a redox cycling toxicant that utilizes molecular oxygen to produce superoxide anion (Zhang et al., 2020a). These effects of PT may act in concert to improve mitochondrial function and protect against hepatic damage in weanling piglets.

The impaired liver function in early-weaned piglets may also have involved ER stress. At weaning, multiple adverse stimuli can create ER stress and result in the accumulation of unfolded and/or misfolded proteins within the ER lumen and subsequent activation of the unfolded protein response (**UPR**) pathways. In the early-weaned piglets, the increased hepatic expression of ER stress markers, such as GRP78, paralleled the pathological alteration of hepatocyte ER structure. Under normal conditions, the UPR sensors (i.e., IRE1α, PERK, and ATF6) are restrained by GRP78 within their intralumenal domains and rendered inactive (Lebeaupin et al., 2018). Upon ER stress, improperly folded proteins compete with the UPR sensors for binding to GRP78, leading to the release of GRP78 from these sensors and they become activated (Lebeaupin et al., 2018). GRP78 is one of the downstream targets of UPR pathways, and its expression is considered a sensitive indicator of ER stress and triggering of the UPR (Lee, 2005).

In the early-weaned piglets, dietary PT supplementation significantly inhibited the expression of hepatic GRP78 at both the mRNA and protein levels. Importantly, PT robustly decreased the expression levels of CHOP and its downstream ERO1A. In the initial phase of ER stress, the UPR serves an adaptive role that can reestablish proteostasis and facilitate cell survival. However, if the adaptive UPR is overwhelmed by prolonged ER stress, it will be switched to a proapoptotic response that is mainly regulated by the UPR components, such as CHOP and ERO1A, and by the cross talk between ER and mitochondria (Calfon et al., 2002; Cao and Kaufman, 2013).

Evidence from both in vitro and in vivo studies has shown that CHOP serves as a potent inducer of ER stress-associated cell death by activating several proapoptotic proteins (Calfon et al., 2002; Malhotra and Kaufman, 2007). CHOP also transcriptionally activates ERO1A, resulting in an exaggerated formation of free radicals and oxidative products in the ER (Wang et al., 1998; Oyadomari and Mori, 2004). ERO1A has been recognized as a major inducer of ER-derived free radicals, as the process of oxidative protein folding involves the generation of one molecule of hydrogen peroxide during the formation of each disulfide bond mediated by ERO1A (Gross et al., 2006). The mechanism underlying CHOP-dependent apoptosis is also related to proapoptotic Ca^{2+} signaling (Cao and Kaufman, 2013). During ER stress, Ca^{2+} released from the ER is taken up by nearby mitochondria and this induces mitochondrial dysfunction, as indicated by the overproduction of superoxide anion and the activation of proapoptotic signals (Cao and Kaufman, 2013).

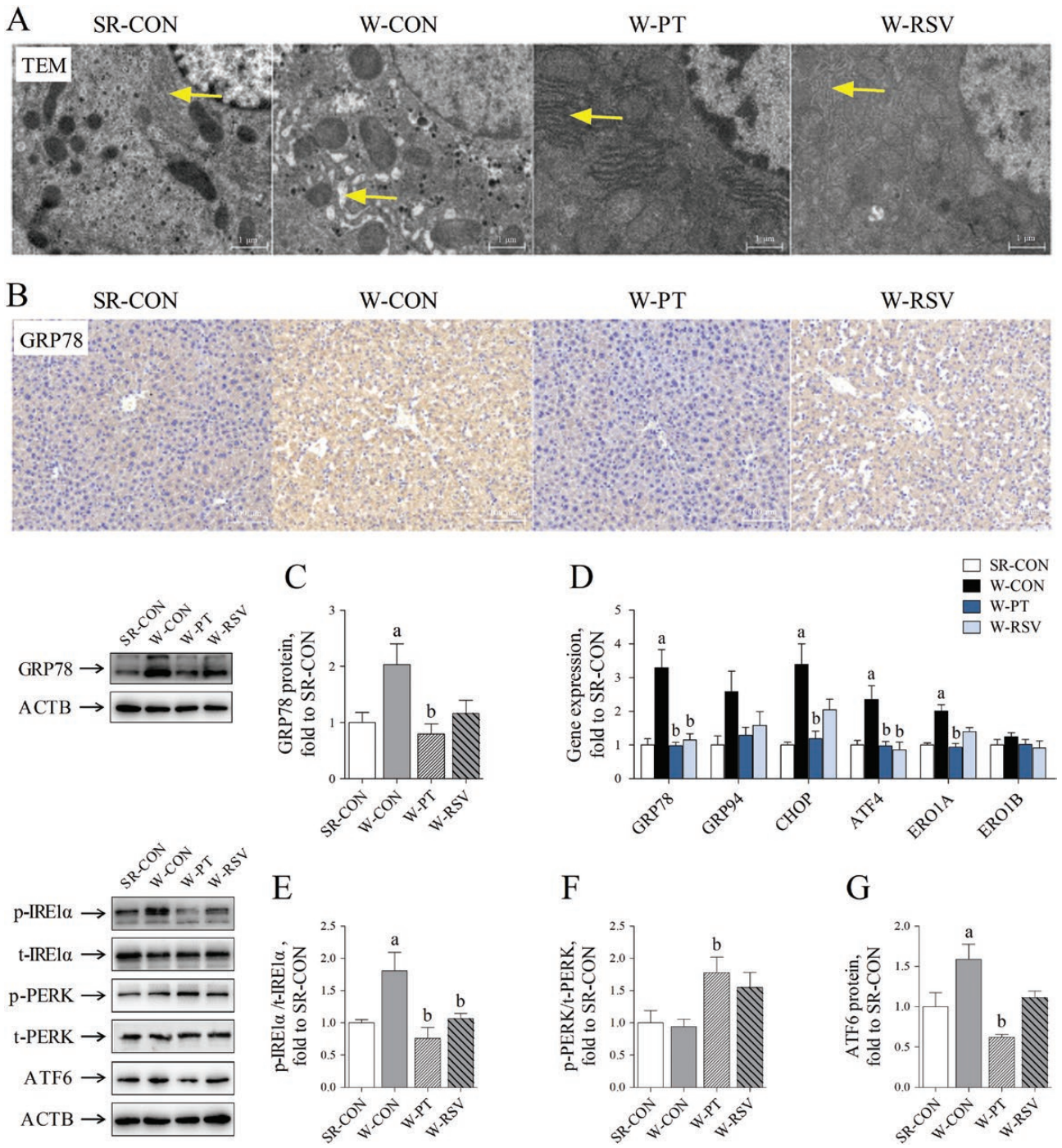

Figure 5. Effects of PT and RSV supplementation on hepatic ER stress and UPR signals in weanling piglets. (A) Representative images of hepatic ultrastructure observed by TEM (5,000× magnification); (B) representative images of GRP78 staining (200× magnification); (C) the expression of hepatic GRP78 protein; (D) activation of ER stress was reflected by the mRNA levels of ER stress-related markers, GRP78, GRP94, CHOP, ATF4, ERO1A, and ERO1B; (E) the phosphorylation of hepatic IRE1α; (F) the phosphorylation of hepatic PERK; and (G) the expression of hepatic ATF6 protein. Values are represented as mean ± SE, $n = 6$. [a]Significant difference compared with SR-CON. [b]Significant difference compared with W-CON.

Therefore, the downregulation of CHOP and ERO1A by PT may contribute to the mitigation of hepatic apoptosis, free radical accumulation, and mitochondrial dysfunction in the early-weaned piglets.

In the current work, PT showed promise for restoring hepatic UPR signals upon ER stress. The administration of PT decreased the phosphorylation of hepatic IRE1α that was dramatically increased by early weaning. Phosphorylated IRE1α has RNase activity and catalyzes the splicing of X-box-binding protein 1 (**XBP1**). The spliced XBP1 (**XBP1s**) initially promotes an adaptive UPR by increasing the protein-folding capacity (Cao and Kaufman, 2013). However, prolonged ER stress shifts XBP1s to transactivate a cluster of apoptotic and inflammatory targets, including CHOP. The expression levels of ATF4 mRNA and ATF6

protein were also reduced after PT treatment, and both of these can transcriptionally activate CHOP during the terminal phase of the UPR (Pagliassotti, 2012). These findings may reflect potential mechanisms that would explain the downregulation of CHOP in the W-PT piglets.

Interestingly, PT increased the phosphorylation of hepatic PERK, an upstream protein kinase of eukaryotic initiation factor 2 alpha (**eIF2α**). Activation of PERK phosphorylates eIF2α at serine residue 51 to initiate a transient cellular translational arrest to mitigate ER workload (Chaudhari et al., 2014). Paradoxically, the phosphorylated eIF2α may also promote a selective synthesis of ATF4 that activates several UPR-related genes, including CHOP (Lebeaupin et al., 2018). PERK can also dissociate the interaction between NRF2 and its inhibitor Kelch-like ECH-associated protein 1 through phosphorylation modification, thereby facilitating the nuclear import of NRF2 for the transcriptional activation of antioxidant and detoxification enzymes (Cullinan et al., 2003). Thus, the activation of PERK may offer a possible explanation for the increased expression of nuclear NRF2 protein in the liver of PT-treated weaned piglets. The NRF2 signals engage survival responses and coordinate the convergence of ER stress with oxidative stress, thereby protecting the cells against free radical-induced oxidative damage and apoptosis (Cullinan and Diehl, 2006).

The benefits of PT in ameliorating ER stress may also be achieved through the activation of SIRT1, which is considered a negative regulator of multiple arms of UPR signaling (Li et al., 2011; Prola et al., 2017; Zhang et al., 2018). Overexpression of SIRT1 in mice increases the resistance of the liver to obesity-induced ER stress by inhibiting IRE-1-dependent splicing of XBP1 (Li et al., 2011). SIRT1 deacetylates XBP1s and represses its transcriptional activity (Wang et al., 2011). Consistently, the activation of SIRT1 by RSV suppresses the expression of IRE1α and its downstream GRP78 and CHOP (Zhang et al., 2018). In addition, SIRT1 inhibits the activity of eIF2α through deacetylation at its lysine residue 143, which in turn decreases the expression of its downstream ATF4 and CHOP (Prola et al., 2017). SIRT1 can also promote the expression of ER chaperones to facilitate protein folding, allowing the cells to tackle an increased demand for protein folding (Jung et al., 2012). These results may explain the decreases in the phosphorylation of IRE1α and the expression levels of ER stress markers observed in the W-PT livers.

In conclusion, this investigation provides insights into the benefits of PT supplementation for mitigating the liver injury induced by early weaning in piglets. PT is more potent than its parent compound RSV in terms of improving mitochondrial function and ER homeostasis, and these effects probably arise through its activation of SIRT1. The findings presented here may help in the development of novel nutrition strategies to ameliorate hepatic dysfunction in early-weaned piglets. Considering the similarities between humans and pigs in anatomy and physiology, the findings obtained here may also provide a number of important clues to improve the liver function and health status in human infants after weaning.

Supplementary Data

Supplementary data are available at *Journal of Animal Science* online.

Acknowledgments

This study was supported by the .National Natural Science Foundation of China (31802094 and 31902197), the Natural Science Foundation of Jiangsu Province (BK20180531), the Postdoctoral Research Foundation of China (2018M632320 and 2019T120436), and the Foundation of Key Laboratory of Veterinary Biotechnology, Shanghai, P. R. China (klab201710).

Conflict of interest statement

The authors declare no conflict of interest.

Literature Cited

Aguirre, L., I. Milton-Laskibar, E. Hijona, L. Bujanda, A. M. Rimando, and M. P. Portillo. 2016. Effects of pterostilbene in brown adipose tissue from obese rats. *J. Physiol. Biochem.* **73**:457–464. doi:10.1007/s13105-017-0556-2

Aquilano, K., P. Vigilanza, S. Baldelli, B. Pagliei, G. Rotilio, and M. R. Ciriolo. 2010. Peroxisome proliferator-activated receptor γ co-activator 1α (PGC-1α) and sirtuin 1 (SIRT1) reside in mitochondria: possible direct function in mitochondrial biogenesis. *J. Biol. Chem.* **285**:21590–21599. doi:10.1074/jbc.M109.070169

Baur, J. A., and D. A. Sinclair. 2006. Therapeutic potential of resveratrol: the in vivo evidence. *Nat. Rev. Drug Discov.* **5**:493–506. doi:10.1038/nrd2060

Bhakkiyalakshmi, E., K. Dineshkumar, S. Karthik, D. Sireesh, W. Hopper, R. Paulmurugan, and K. M. Ramkumar. 2016. Pterostilbene-mediated Nrf2 activation: mechanistic insights on Keap1: Nrf2 interface. *Bioorg. Med. Chem.* **24**:3378–3386. doi:10.1016/j.bmc.2016.05.011

Brenmoehl, J., and A. Hoeflich. 2013. Dual control of mitochondrial biogenesis by sirtuin 1 and sirtuin 3. *Mitochondrion* **13**:755–761. doi:10.1016/j.mito.2013.04.002

Calfon, M., H. Zeng, F. Urano, J. H. Till, S. R. Hubbard, H. P. Harding, S. G. Clark, and D. Ron. 2002. IRE1 couples endoplasmic reticulum load to secretory capacity by processing the XBP-1 mRNA. *Nature* **415**:92–96. doi:10.1038/415092a

Campbell, J. M., J. D. Crenshaw, and J. Polo. 2013. The biological stress of early weaned piglets. *J. Anim. Sci. Biotechnol.* **4**:19. doi:10.1186/2049-1891-4-19

Cao, S. S., and R. J. Kaufman. 2013. Targeting endoplasmic reticulum stress in metabolic disease. *Expert Opin. Ther. Targets* **17**:437–448. doi:10.1517/14728222.2013.756471

Chang, H. C., and L. Guarente. 2014. SIRT1 and other sirtuins in metabolism. *Trends Endocrinol. Metab.* **25**:138–145. doi:10.1016/j.tem.2013.12.001

Chaudhari, N., P. Talwar, A. Parimisetty, C. Lefebvre d'Hellencourt, and P. Ravanan. 2014. A molecular web: endoplasmic reticulum stress, inflammation, and oxidative stress. *Front. Cell. Neurosci.* **8**:213. doi:10.3389/fncel.2014.00213

Cheng, Y., S. Di, C. Fan, L. Cai, C. Gao, P. Jiang, W. Hu, Z. Ma, S. Jiang, Y. Dong, *et al.* 2016. SIRT1 activation by pterostilbene attenuates the skeletal muscle oxidative stress injury and mitochondrial dysfunction induced by ischemia reperfusion injury. *Apoptosis* **21**:905–916. doi:10.1007/s10495-016-1258-x

Chiou, Y. S., M. L. Tsai, K. Nagabhushanam, Y. J. Wang, C. H. Wu, C. T. Ho, and M. H. Pan. 2011. Pterostilbene is more potent than resveratrol in preventing azoxymethane (AOM)-induced colon tumorigenesis via activation of the NF-E2-related factor 2 (Nrf2)-mediated antioxidant signaling pathway. *J. Agric. Food Chem.* **9**:2725–2733. doi:10.1021/jf2000103

Choo, Q. Y., S. C. M. Yeo, P. C. Ho, Y. Tanaka, and H. S. Lin. 2014. Pterostilbene surpassed resveratrol for anti-inflammatory application: potency consideration and pharmacokinetics perspective. *J. Funct. Foods* **11**:352–362. doi:10.1016/j.jff.2014.10.018

Cullinan, S. B., and J. A. Diehl. 2006. Coordination of ER and oxidative stress signaling: the PERK/Nrf2 signaling pathway. *Int. J. Biochem. Cell Biol.* **8**:317–332. doi:10.1016/j.biocel.2005.09.018

Cullinan, S. B., D. Zhang, M. Hannink, E. Arvisais, R. J. Kaufman, and J. A. Diehl. 2003. Nrf2 is a direct PERK substrate and effector of PERK-dependent cell survival. *Mol. Cell. Biol.* **23**:7198–7209. doi:10.1128/mcb.23.20.7198-7209.2003

Gan, Z., W. Wei, J. Wu, Y. Zhao, L. Zhang, T. Wang, and X. Zhong. 2019. Resveratrol and curcumin improve intestinal mucosal integrity and decrease m6A RNA methylation in the intestine of weaning piglets. *ACS Omega* **4**:17438–17446. doi:10.1021/acsomega.9b02236

Gross, E., C. S. Sevier, N. Heldman, E. Vitu, M. Bentzur, C. A. Kaiser, C. Thorpe, and D. Fass. 2006. Generating disulfides enzymatically: reaction products and electron acceptors of the endoplasmic reticulum thiol oxidase Ero1p. *Proc. Natl. Acad. Sci. U. S. A.* **103**:299–304. doi:10.1073/pnas.0506448103

Guo, Y., L. Zhang, F. Li, C. P. Hu, and Z. Zhang. 2016. Restoration of sirt1 function by pterostilbene attenuates hypoxia-reoxygenation injury in cardiomyocytes. *Eur. J. Pharmacol.* **776**:26–33. doi:10.1016/j.ejphar.2016.02.052

Hubbard, B. P., A. P. Gomes, H. Dai, J. Li, A. W. Case, T. Considine, T. V. Riera, J. E. Lee, S. Y. E, D. W. Lamming, *et al.* 2013. Evidence for a common mechanism of SIRT1 regulation by allosteric activators. *Science* **339**:1216–1219. doi:10.1126/science.1231097

Jung, T. W., K. T. Lee, M. W. Lee, and K. H. Ka. 2012. SIRT1 attenuates palmitate-induced endoplasmic reticulum stress and insulin resistance in HepG2 cells via induction of oxygen-regulated protein 150. *Biochem. Biophys. Res. Commun.* **422**:229–232. doi:10.1016/j.bbrc.2012.04.129

Kang, D., S. H. Kim, and N. Hamasaki. 2007. Mitochondrial transcription factor A (TFAM): roles in maintenance of mtDNA and cellular functions. *Mitochondrion* **7**:39–44. doi:10.1016/j.mito.2006.11.017

Korla, K. 2016. Reactive oxygen species and energy machinery: an integrated dynamic model. *J. Biomol. Struct. Dyn.* **34**:1625–1640. doi:10.1080/07391102.2015.1086958

Kosuru, R., V. Kandula, U. Rai, S. Prakash, Z. Xia, and S. Singh. 2018. Pterostilbene decreases cardiac oxidative stress and inflammation via activation of AMPK/Nrf2/HO-1 pathway in fructose-fed diabetic rats. *Cardiovasc. Drugs Ther.* **32**:147–163. doi:10.1007/s10557-018-6780-3

Lebeaupin, C., D. Vallée, Y. Hazari, C. Hetz, E. Chevet, and B. Bailly-Maitre. 2018. Endoplasmic reticulum stress signalling and the pathogenesis of non-alcoholic fatty liver disease. *J. Hepatol.* **69**:927–947. doi:10.1016/j.jhep.2018.06.008

Lee, A. S. 2005. The ER chaperone and signaling regulator GRP78/BiP as a monitor of endoplasmic reticulum stress. *Methods* **35**:373–381. doi:10.1016/j.ymeth.2004.10.010

Leone, T. C., C. J. Weinheimer, and D. P. Kelly. 1999. A critical role for the peroxisome proliferator-activated receptor alpha (PPARalpha) in the cellular fasting response: the PPARalpha-null mouse as a model of fatty acid oxidation disorders. *Proc. Natl. Acad. Sci. U. S. A.* **96**:7473–7478. doi:10.1073/pnas.96.13.7473

Li, Y., S. Xu, A. Giles, K. Nakamura, J. W. Lee, X. Hou, G. Donmez, J. Li, Z. Luo, K. Walsh, *et al.* 2011. Hepatic overexpression of SIRT1 in mice attenuates endoplasmic reticulum stress and insulin resistance in the liver. *FASEB J.* **25**:1664–1679. doi:10.1096/fj.10-173492

Liu, D., Z. Ma, L. Xu, X. Zhang, S. Qiao, and J. Yuan. 2019. PGC1α activation by pterostilbene ameliorates acute doxorubicin cardiotoxicity by reducing oxidative stress via enhancing AMPK and SIRT1 cascades. *Aging (Albany. NY)*. **11**:10061–10073. doi:10.18632/aging.102418

Liu, X., X. Yang, L. Han, F. Ye, M. Liu, W. Fan, K. Zhang, Y. Kong, J. Zhang, L. Shi, *et al.* 2017. Pterostilbene alleviates polymicrobial sepsis-induced liver injury: possible role of SIRT1 signaling. *Int. Immunopharmacol.* **49**:50–59. doi:10.1016/j.intimp.2017.05.022

Livak, K. J., and T. D. Schmittgen. 2001. Analysis of relative gene expression data using real-time quantitative PCR and the 2(-Delta Delta C(T)) Method. *Methods* **25**:402–408. doi:10.1006/meth.2001.1262

Luo, Z., W. Zhu, Q. Guo, W. Luo, J. Zhang, W. Xu, and J. Xu. 2016. Weaning induced hepatic oxidative stress, apoptosis, and aminotransferases through MAPK signaling pathways in piglets. *Oxid. Med. Cell Longev.* **2016**:4768541. doi:10.1155/2016/4768541

Malhotra, J. D., and R. J. Kaufman. 2007. Endoplasmic reticulum stress and oxidative stress: a vicious cycle or a double-edged sword? *Antioxid. Redox Signal.* **9**:2277–2293. doi:10.1089/ars.2007.1782

Mizuno, C. S., G. Ma, S. I. Khan, A. Patny, M. A. Avery, and A. M. Rimando. 2008. Design, synthesis, biological evaluation and docking studies of pterostilbene analogs inside PPARα. *Bioorgan. Med. Chem.* **16**:3800–3808. doi:10.1016/j.bmc.2008.01.051

Nagao, K., T. Jinnouchi, S. Kai, and T. Yanagita. 2017. Pterostilbene, a dimethylated analog of resveratrol, promotes energy metabolism in obese rats. *J. Nutr. Biochem.* **43**:151–155. doi:10.1016/j.jnutbio.2017.02.009

Naik, B., A. Nirwane, and A. Majumdar. 2017. Pterostilbene ameliorates intracerebroventricular streptozotocin induced memory decline in rats. *Cogn. Neurodyn.* **11**:35–49. doi:10.1007/s11571-016-9413-1

Nakamura, M. T., B. E. Yudell, and J. J. Loor. 2014. Regulation of energy metabolism by long-chain fatty acids. *Prog. Lipid Res.* **53**:124–144. doi:10.1016/j.plipres.2013.12.001

Nirwane, A., and A. Majumdar. 2016. Resveratrol and pterostilbene ameliorate the metabolic derangements associated with smokeless tobacco in estrogen deficient female rats. *J. Funct. Foods* **23**:261–277. doi:10.1016/j.jff.2015.12.030

Novais, A. K., Y. Martel-Kennes, C. Roy, K. Deschêne, S. Beaulieu, N. Bergeron, J. P. Laforest, M. Lessard, J. J. Matte, and J. Lapointe. 2020. Tissue-specific profiling reveals modulation of cellular and mitochondrial oxidative stress in normal- and low-birth weight piglets throughout the peri-weaning period. *Animal* **14**:1014–1024. doi:10.1017/S1751731119002829

Oyadomari, S., and M. Mori. 2004. Roles of CHOP/GADD153 in endoplasmic reticulum stress. *Cell Death Differ.* **11**:381–389. doi:10.1038/sj.cdd.4401373

Pagliassotti, M. J. 2012. Endoplasmic reticulum stress in nonalcoholic fatty liver disease. *Annu. Rev. Nutr.* **32**:17–33. doi:10.1146/annurev-nutr-071811-150644

Pike, L. S., A. L. Smift, N. J. Croteau, D. A. Ferrick, and M. Wu. 2011. Inhibition of fatty acid oxidation by etomoxir impairs NADPH production and increases reactive oxygen species resulting in ATP depletion and cell death in human glioblastoma cells. *Biochim. Biophys. Acta* **1807**:726–734. doi:10.1016/j.bbabio.2010.10.022

Price, N. L., A. P. Gomes, A. J. Ling, F. V. Duarte, A. Martin-Montalvo, B. J. North, B. Agarwal, L. Ye, G. Ramadori, J. S. Teodoro, *et al.* 2012. SIRT1 is required for AMPK activation and the beneficial effects of resveratrol on mitochondrial function. *Cell Metab.* **15**:675–690. doi:10.1016/j.cmet.2012.04.003

Prola, A., J. Pires Da Silva, A. Guilbert, L. Lecru, J. Piquereau, M. Ribeiro, P. Mateo, M. Gressette, D. Fortin, C. Boursier, *et al.* 2017. SIRT1 protects the heart from ER stress-induced cell death through eIF2α deacetylation. *Cell Death Differ.* **24**:343–356. doi:10.1038/cdd.2016.138

Rauf, A., M. Imran, H. A. R. Suleria, B. Ahmad, D. G. Peters, and M. S. Mubarak. 2017. A comprehensive review of the health perspectives of resveratrol. *Food Funct.* **8**:4284–4305. doi:10.1039/c7fo01300k

Seki, E., and B. Schnabl. 2012. Role of innate immunity and the microbiota in liver fibrosis: crosstalk between the liver and gut. *J. Physiol.* **590**:447–458. doi:10.1113/jphysiol.2011.219691

Shen, W., K. Liu, C. Tian, L. Yang, X. Li, J. Ren, L. Packer, C. W. Cotman, and J. Liu. 2008. R-alpha-lipoic acid and acetyl-L-carnitine complementarily promote mitochondrial biogenesis in murine 3T3-L1 adipocytes. *Diabetologia* **51**:165–174. doi:10.1007/s00125-007-0852-4

Song, L., T. Chen, X. Zhao, Q. Xu, R. Jiao, J. Li, and L. Kong. 2019. Pterostilbene prevents hepatocyte epithelial-mesenchymal transition in fructose-induced liver fibrosis through suppressing miR-34a/Sirt1/p53 and TGF-β1/Smads signaling. *Br. J. Pharmacol.* **176**:1619–1634. doi:10.1111/bph.14573

Sutherland, M. A., S. R. Niekamp, S. L. Rodriguez-Zas, and J. L. Salak-Johnson. 2006. Impacts of chronic stress and social status on various physiological and performance measures in pigs of different breeds. *J. Anim. Sci.* **84**:588–596. doi:10.2527/2006.843588x

Vladislav, E., K. Dana, and K. Jaroslav. 2006. Comparative study of natural antioxidants–curcumin, resveratrol and melatonin–in cadmium-induced oxidative damage in mice. *Toxicology* **225**:150–156. doi:10.1016/j.tox.2006.05.011

Vollmar, B., and M. D. Menger. 2009. The hepatic microcirculation: mechanistic contributions and therapeutic targets in liver injury and repair. *Physiol. Rev.* **89**:1269–1339. doi:10.1152/physrev.00027.2008

Wang, F. M., Y. J. Chen, and H. J. Ouyang. 2011. Regulation of unfolded protein response modulator XBP1s by acetylation and deacetylation. *Biochem. J.* **433**:245–252. doi:10.1042/BJ20101293

Wang, X. Z., M. Kuroda, J. Sok, N. Batchvarova, R. Kimmel, P. Chung, H. Zinszner, and D. Ron. 1998. Identification of novel stress-induced genes downstream of chop. *EMBO J.* **17**:3619–3630. doi:10.1093/emboj/17.13.3619

Wu, W., X. Ding, T. Gu, W. Guo, R. Jiao, L. Song, Y. Sun, Y. Pan, and L. Kong. 2020. Pterostilbene improves hepatic lipid accumulation via the MiR-34a/Sirt1/SREBP-1 pathway in fructose-fed rats. *J. Agric. Food Chem.* **68**:1436–1446. doi:10.1021/acs.jafc.9b04259

Wu, Y. T., S. B. Wu, and Y. H. Wei. 2014. Roles of sirtuins in the regulation of antioxidant defense and bioenergetic function of mitochondria under oxidative stress. *Free Radic. Res.* **48**:1070–1084. doi:10.3109/10715762.2014.920956

Yang, Y., C. Fan, B. Wang, Z. Ma, D. Wang, B. Gong, S. Di, S. Jiang, Y. Li, T. Li, *et al.* 2017. Pterostilbene attenuates high glucose-induced oxidative injury in hippocampal neuronal cells by activating nuclear factor erythroid 2-related factor 2. *Biochim. Biophys. Acta Mol. Basis Dis.* **1863**:827–837. doi:10.1016/j.bbadis.2017.01.005

Yang, C., B. Ko, C. T. Hensley, L. Jiang, A. T. Wasti, J. Kim, J. Sudderth, M. Calvaruso, L. Lumata, M. A. Mitsche, *et al.* 2014. Glutamine oxidation maintains the TCA cycle and cell survival during impaired mitochondrial pyruvate transport. *Mol. Cell* **56**:414–424. doi:10.1016/j.molcel.2014.09.025

Yang, Y., J. Wang, Y. Li, C. Fan, S. Jiang, L. Zhao, S. Di, Z. Xin, B. Wang, G. Wu, *et al.* 2016. HO-1 signaling activation by pterostilbene treatment attenuates mitochondrial oxidative damage induced by cerebral ischemia reperfusion injury. *Mol. Neurobiol.* **53**:2339–2353. doi:10.1007/s12035-015-9194-2

Yeo, S. C., P. C. Ho, and H. S. Lin. 2013. Pharmacokinetics of pterostilbene in Sprague–Dawley rats: the impacts of aqueous solubility, fasting, dose escalation, and dosing route on bioavailability. *Mol. Nutr. Food Res.* **57**:1015–1025. doi:10.1002/mnfr.201200651

Yin, J., M. M. Wu, H. Xiao, W. K. Ren, J. L. Duan, G. Yang, T. J. Li, and Y. L. Yin. 2014. Development of an antioxidant system after early weaning in piglets. *J. Anim. Sci.* **92**:612–619. doi:10.2527/jas.2013-6986

Yueh, M. F., K. Taniguchi, S. Chen, R. M. Evans, B. D. Hammock, M. Karin, and R. H. Tukey. 2014. The commonly used antimicrobial additive triclosan is a liver tumor promoter. *Proc. Natl. Acad. Sci. U. S. A.* **111**:17200–17205. doi:10.1073/pnas.1419119111

Zhang, L., D. Bao, P. Li, Z. Lu, L. Pang, Z. Chen, H. Guo, Z. Gao, and Q. Jin. 2018. Particle-induced SIRT1 downregulation promotes osteoclastogenesis and osteolysis through ER stress regulation. *Biomed. Pharmacother.* **104**:300–306. doi:10.1016/j.biopha.2018.05.030

Zhang, H., Y. Chen, Y. Chen, S. Ji, P. Jia, Y. Li, T. Wang. 2020b. Comparison of the protective effects of resveratrol and pterostilbene against intestinal damage and redox imbalance in weanling piglets. *J. Anim. Sci. Biotechnol.* **11**:52. doi:10.1016/j.biopha.2018.05.030

Zhang, H., Y. Chen, Y. Chen, P. Jia, S. Ji, J. Xu, Y. Li, and T. Wang. 2020a. Comparison of the effects of resveratrol and its derivative pterostilbene on hepatic oxidative stress and mitochondrial dysfunction in piglets challenged with diquat. *Food Funct.* **11**:4202–4215. doi:10.1039/d0fo00732c

Zhang, C., J. Luo, B. Yu, P. Zheng, Z. Huang, X. Mao, J. He, J. Yu, J. Chen, and D. Chen. 2015. Dietary resveratrol supplementation improves meat quality of finishing pigs through changing muscle fiber characteristics and antioxidative status. *Meat Sci.* **102**:15–21. doi:10.1016/j.meatsci.2014.11.014

Zhao, H. T., S. Kalivendi, H. Zhang, J. Joseph, K. Nithipatikom, J. Vasquez-Vivar, and B. Kalyanaraman. 2003. Superoxide reacts with hydroethidine but forms a fluorescent product that is distinctly different from ethidium: potential implications in intracellular fluorescence detection of superoxide. *Free Radic. Biol. Med.* **34**:1359–1368. doi:10.1016/s0891-5849(03)00142-4

Zheng, J., W. Liu, X. Zhu, L. Ran, H. Lang, L. Yi, M. Mi, and J. Zhu. 2020. Pterostilbene enhances endurance capacity via promoting skeletal muscle adaptations to exercise training in rats. *Molecules* **25**:186. doi:10.3390/molecules25010186

Zhu, L. H., K. L. Zhao, X. L. Chen, and J. X. Xu. 2012. Impact of weaning and an antioxidant blend on intestinal barrier function and antioxidant status in pigs. *J. Anim. Sci.* **90**:2581–2589. doi:10.2527/jas.2011-4444